LAWRENCE
LIVERMORE
NATIONAL
LABORATORY

LLNL-CONF-523631

SIMULATION OF HYDRAULIC FRACTURE NETWORKS IN THREE DIMENSIONS

R. R. Settgast, S. M. Johnson, P. Fu, S. Walsh, F. Ryerson

January 22, 2012

Stanford Geothermal Workshop
Stanford, CA, United States
January 30, 2012 through February 1, 2012

Disclaimer

This document was prepared as an account of work sponsored by an agency of the United States government. Neither the United States government nor Lawrence Livermore National Security, LLC, nor any of their employees makes any warranty, expressed or implied, or assumes any legal liability or responsibility for the accuracy, completeness, or usefulness of any information, apparatus, product, or process disclosed, or represents that its use would not infringe privately owned rights. Reference herein to any specific commercial product, process, or service by trade name, trademark, manufacturer, or otherwise does not necessarily constitute or imply its endorsement, recommendation, or favoring by the United States government or Lawrence Livermore National Security, LLC. The views and opinions of authors expressed herein do not necessarily state or reflect those of the United States government or Lawrence Livermore National Security, LLC, and shall not be used for advertising or product endorsement purposes.

PROCEEDINGS, Thirty-Seventh Workshop on Geothermal Reservoir Engineering
Stanford University, Stanford, California, January 30 - February 1, 2012
SGP-TR-194

SIMULATION OF HYDRAULIC FRACTURE NETWORKS IN THREE DIMENSIONS

Randolph Settgast, Scott Johnson, Pengcheng Fu, Stuart D.C. Walsh, Frederick Ryerson

Atmospheric, Earth, and Energy Division, Lawrence Livermore National Laboratory
7000 East Ave., L-286
Livermore, CA 94550, USA
e-mail: settgast1@llnl.gov

ABSTRACT

Hydraulic fracturing has been an enabling technology for commercially stimulating fracture networks for over half of a century. It has become one of the most widespread technologies for engineering subsurface fracture systems. Despite the ubiquity of this technique in the field, understanding and prediction of the hydraulic induced propagation of the fracture network in realistic, heterogeneous reservoirs has been limited. Recent developments allowing the modeling of complex fracture propagation and advances in quantifying solution uncertainties, provide the possibility of capturing both the fracturing behavior and longer term permeability evolution of rock masses under hydraulic loading across both dynamic and viscosity dominated regimes. We present a framework for leveraging these advances in practical workflows for analyzing prospective and operating geothermal / hydrothermal sites. We will demonstrate the first phase of this effort through illustrations of fully three-dimensional, tightly coupled hydromechanical simulations of hydraulically induced fracture network propagation and discuss preliminary results regarding the mechanisms by which fracture interactions and the accompanying changes to the stress field can lead to deleterious or beneficial changes to the fracture network.

This work was performed under the auspices of the U.S. Department of Energy by Lawrence Livermore National Laboratory under Contract DE-AC52-07NA27344.

INTRODUCTION

Reservoir stimulation through hydraulic fracture is a critical element in unlocking the potential of geothermal energy production where natural permeability is inadequate (Figure 1). However, despite the fact that hydraulic fracturing has been in employed for almost 60 years, having first been used to simulate oil and gas wells in the early 1950's, many uncertainties still surround its use. In particular, given the public scrutiny of hydraulic fracture operations due to concerns regarding its environmental impact and potential for induced seismicity, there is a need for robust models capable of determining:

- The impact of hydraulic fracturing on caprock integrity;
- Whether fractures will propagate as designed;
- What seismicity will be induced as a result of the fracturing operation;
- Whether recovered fluids will be released; and importantly,
- Whether production rates will meet expectations.

Addressing these questions is a difficult task. Modeling hydraulic fracturing in the presence of a natural fracture network is a complicated multi-physics, multi-scale problem due to the coupling between fluid, rock matrix, and rock joints, as well as the interactions between propagating new fractures and existing natural fractures. Nevertheless, in recent years, a number of advances have allowed researchers in related fields to tackle the modeling of complex fracture propagation as well as the mechanics of heterogeneous systems. These developments, combined with advances in quantifying solution uncertainties, provide possibilities for the geologic modeling community to capture both the fracturing behavior and longer term permeability evolution of rock masses under hydraulic loading across both dynamic and viscosity dominated regimes.

This paper describes the development of a computational capability focused on the creation, characterization, maintenance, and active management of optimal fracture networks for energy extraction from enhanced geothermal systems. The primary component of this capability is the development of a high-fidelity geomechanics code, GEOS, a multi-scale, multi-physics, fracture mechanics model that will describe the development

of fracture networks for different lithologies and applications as a function of initial geologic conditions, regional stress and stimulation work flows. Here we present the first phase of this effort through illustrations of fully three-dimensional, tightly coupled hydromechanical simulations of hydraulically induced fracture network propagation and discuss preliminary results regarding the mechanisms by which fracture interactions and the accompanying changes to the stress field can lead to deleterious or beneficial changes to the fracture network.

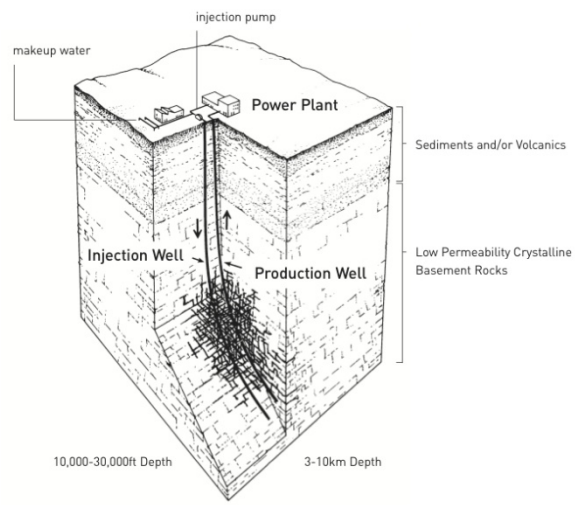

Figure 1: Schematic of an Enhanced Geothermal System with injection and production wells extracting heat from a stimulated volume of rock with low initial permeability [1].

MECHANICS AND FLOW

Mechanics

In this work, the deformation of meshed volumes is governed by a series of standard Lagrangian FEM solvers. Fundamentally these solvers enforce some form of the equations of motion

$$\nabla \cdot \mathbf{T} + \rho\left(\mathbf{b} - \mathbf{a}\right) = \mathbf{0}. \tag{1}$$

Depending on the application, (1) can take the form of a general mechanics solution, a static solution (**a**=**0**), as well as being cast in terms of first or second Piola-Kirchhoff tensors. In the cases presented here, an explicit dynamics solver is applied to the first Piola-Kirchhoff forms of (1).

Parallel Plate Flow

The flow of the fluid through the fractures is assumed adhere to the parallel plate flow assumptions [2,3]. Given a single edge connected to n faces where each face is given a local index i. To solve for the flow, we calculate the mass flux between the edge and each face. The fracture permeability of between the face and the edge κ_i is given as

$$\kappa_i = \frac{\alpha_i^3 w}{12\mu L_i}, \tag{1}$$

where α_i is the hydraulic aperture of the face, w is the length of the edge, μ is the dynamic viscosity, and L_i is the length from the center of the face to the center of the edge. The mass flow rate ($\dot{m}_i$) from the face to the edge is easily expressed as

$$\dot{m}_i = \kappa_i\left(\rho_i P_i - \rho_e P_e\right), \tag{2}$$

where ρ_i is the density of the face, P_i is the fluid pressure on the face, ρ_e is the density at the edge, and P_e is the pressure at the edge. Applying conservation of mass at the edge provides a solution of $\rho_e P_e$ as

$$\rho_e P_e = \frac{\sum_i^n \kappa_i \rho_i P_i}{\sum_i^n \kappa_i}. \tag{3}$$

Substituting (3) into (2) allows for the solution of the mass flux between the edge and the face. These relations (1-3) are implemented in both a time explicit transient solver, and a steady-state implicit solver.

FRACTURE

The focus of this work to date is to provide the topological flexibility to model the creation of new surfaces. To this end, tools for splitting a mesh similar to those described by Settgast[4] have been further developed in the GEOS framework. In this approach, nodes, edges, and faces are split along element boundaries into separate entities. This is achieved when a closed path of faces that have attained a ruptured state can be found. This method of splitting along element boundaries is performed on a node-by-node basis and can be described through the following list of procedures:

1. Determine the state on faces, and mark the faces that have achieved a ruptured state.
2. For each node, find a closed path of faces that make up a "rupture plane" about which the node can be split.
3. Split the node, any edges and faces.
4. Repair connectivity between the nodes, edges, faces, and elements.

With the preceding, the application of computational fracture mechanics is feasible. There are many methods by which to attempt this ranging from various cohesive zone approaches [4-6]. In this study

we do not yet apply any of these methods, instead the mesh is simply broken, extending the fracture in the process. The implementation of a method for smooth crack opening will be pursued in future work.

In the case of field scale studies, the mesh resolution required to resolve the stress field near the tip of a fracture is unattainable without some form of automatic mesh refinement near the tip. In cases where this is the case, methods may be used to estimate the stress field as given in [7]. If no such method is utilized, then a stress criteria for face rupture will likely be a compressive stress, as the unbounded stress field is dramatically under-estimated by the resolution.

SURFACE CONTACT

Once fracture surfaces have been generated, they must be prevented from subsequent inter-penetration. In the general case, a contact methodology that allows for shear slip along the surfaces is desired. The general contact enforcement method in GEOS is a variation of the so-called "common-plane" (CP) method. The CP method institutes face-to-face contact by detecting overlapping face geometries, and producing a penalty force resisting the contact. This approach is essentially described in described in [8], although refinements and modifications have been made.

An alternative to the generalized approach, which bears significant computational cost, a simple method of surface contact enforcement is available when no shear slip is present. In this case, a penalty stiffness is enforced on the inter-penetration distance of formerly coincident faces (i.e. faces that used to be the same face prior to rupture). This method is used in the work presented in this study.

COUPLED MECHANICS/FRACTURE/FLOW

The coupling of mechanics solver with fracture capability to a fluid solver to represent the flow through the fractures is relatively straightforward. The first step is to define the flow mesh once the volumetric mesh is split. While there are many options for this, the method presented here is to define the flow mesh on the original faces/edges/nodes that have been split. While these objects are likely to be disconnected from each other, an alternate connectivity that links the original edges to the original faces (recall that these relations have been changed by the fracture process) can be used to define a contiguous mesh as far as the flow solver is concerned.

Once a flow mesh is defined we focus on the method to couple the two solvers together. In essence the procedure for a time-explicit coupled solver is as follows:

1. Perform flow solve using beginning of step apertures, and fluid pressures. This gives the mass in each fluid volume at the end of the step.
$$FluidSolve(P^n, \alpha^n) \Rightarrow m^{n+1}$$
2. Update nodal velocities to mid-step, and displacements to end-of-step.
$$\mathbf{v}^{n+1/2} = \mathbf{v}^{n-1/2} + \mathbf{a}^n \Delta t^n$$
$$\mathbf{u}^{n+1} = \mathbf{u}^n + \mathbf{v}^{n+1/2} \Delta t^{n+1/2}$$
3. Update material state of the solid volume, and generate nodal forces from those volumes.
$$MatUpdt\left(\frac{\partial \mathbf{v}^{n+1/2}}{\partial \mathbf{x}^{n+1/2}}, Q^n, \Delta t^{n+1/2}\right) \Rightarrow Q^{n+1}$$
4. Update the fluid pressure using the mass from step 1, and the volume at the end of the step. Specifically volume is the gap between the physical faces multiplied by the face area.
$$EOS\left(m^{n+1}, V^{n+1}\right) \Rightarrow P^{n+1}$$
5. Apply fluid pressure from a flow face as a boundary condition on the physical faces that are related to it. This is a simple pressure boundary condition to the mechanics solver.
6. Calculate the acceleration of the nodes at the end of the step.

EXAMPLES

In the following examples, a linear elastic material is used for solid materials, and a simple linear equation of state is used for the fluid. The material properties are summarized in Table 1.

Table 1: Summary of Material properties.

Property	Value
Solid Bulk Modulus	15.0 GPa
Solid Shear Modulus	15.0 GPa
Fluid Bulk Modulus	0.1 GPa
Fluid Pressure	7.0 MPa
Min Horizontal Confinement	6.0 MPa
Max Horizontal Confinement	8.0 MPa
Vertical Confinement	10.0 MPa
Dynamic Viscosity (*k*)	1.0e-3 N s/m^2
Rupture Stress Criteria*	5.2 MPa

* note that the compressive value of rupture stress criteria is due to the under-resolution of the mesh, as discussed in the preceding section of fracture.

The first example is a pseudo-2d representation of a horizontal plane (200m x 200m) with a 3 pre-existing

fractures. The middle fracture runs perpendicular to the minimum principle stress, while the end fractures run in the direction of maximum horizontal principle stress as shown in Figure 1. The middle fracture is then pressured at its center, and a "tensile" stress develops at the crack tip as shown in Figure 1b. As shown in the middle figure, the fracture propagates until it joins with the end fractures. At this point the end fractures are pressurized (Figure 1c) and the simulation is terminated.

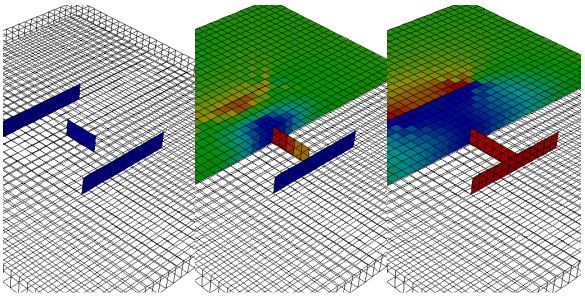

Figure 2: Hydraulically induced extension of a pre-existing fracture terminating on a perpendicular fault using on a pseudo-2d problem. Color scale indicates pressure, and stress in the minimum horizontal direction.

The next example is the 3-dimensional hydraulic fracture propagation in a (200m x 200m x 200m) block. As was the case in the last example, a single fracture runs in the direction of minimum horizontal stress. In this case however, only a single fracture exists in the direction maximum horizontal stress. When the fracture is pressurized, the fracture adopts a circular shape, and begins to extend maintaining its shape. As expected, when the growing fracture joins with a pre-existing perpendicular fracture, growth ceases, and does not restart until both fractures are pressurized – at which point they begin to grow together.

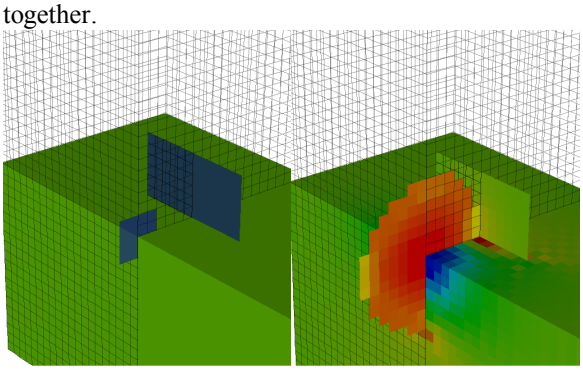

Figure 3: Hydraulically induced extension of a pre-existing fracture terminating on a perpendicular fault using on a 3-dimensional problem. Color scale indicates pressure, and stress in the minimum horizontal direction.

While the preceding examples are a good illustration of rudimentary capabilities and allow for understanding the mechanisms at play during fracture propagation, our end goal is to model the stimulation of a large scale fracture network in 3-dimensions, as was done in 2-dimensions in [9]. While the capability for modeling this problem is remains under development, initial progress has been made. In the following example, a flow calculation is performed on the same 200m block with a pre-existing 3-dimensional joint set as shown in Figure 3. A well source is placed in the lower near corner, while a recovery well is placed in the upper far corner. The source well pressure is specified as 7 MPa, the recovery well pressure is specified as 5 MPa, and hydraulic aperture is fixed at 10 μm.

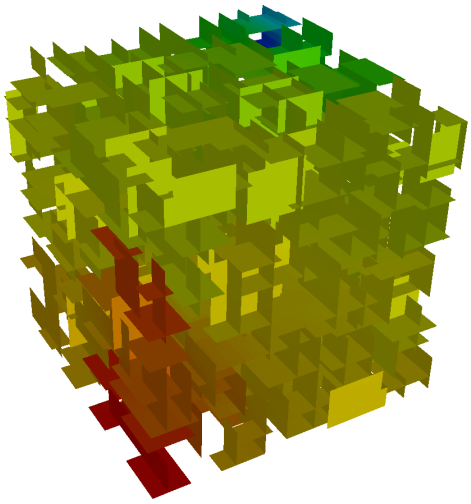

Figure 4: Flow calculation between a source and extraction well on block with a 3-dimensional joint set. Color scale indicates fluid pressure.

CONCLUSIONS AND DIRECTION OF FUTURE WORK

In this study a methodology to simulate the evolution of fracture networks in 3-dimensions through a tightly coupled finite element approach has been presented. Simple examples of hydraulically driven fracture, including the ability to join fractures has been shown. In addition, a simulation of flow through a set of three-dimensional fractures has been shown. While the basic capabilities are promising, additional capabilities are required to achieve the goals of simulation of realistic fracture networks shown in Figure 5. To this end, future work seeks to develop and implement the following:

1. Implementation of quadratic tetrahedral elements for greater flexibility in fracture propagation direction.
2. Development and implementation of a method to estimate crack-tip stresses in 3-dimensions.
3. Implementation of an AMR capability to greater resolve the material states at the crack-tips.
4. A complete suite of implicit and explicit solvers to address different time scales, and the ability to transition between scales automatically.

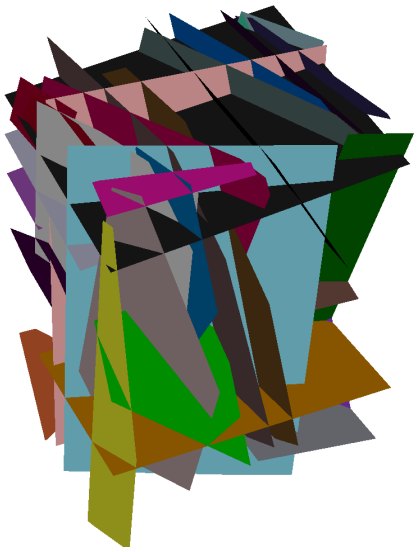

Figure 5: A realistic fault set derived from experimental data [10].

ACKNOWLEDGMENTS

This document was prepared as an account of work sponsored by an agency of the United States government. Neither the United States government nor Lawrence Livermore National Security, LLC, nor any of their employees makes any warranty, expressed or implied, or assumes any legal liability or responsibility for the accuracy, completeness, or usefulness of any information, apparatus, product, or process disclosed, or represents that its use would not infringe privately owned rights. Reference herein to any specific commercial product, process, or service by trade name, trademark, manufacturer, or otherwise does not necessarily constitute or imply its endorsement, recommendation, or favoring by the United States government or Lawrence Livermore National Security, LLC. The views and opinions of authors expressed herein do not necessarily state or reflect those of the United States government or Lawrence Livermore National Security, LLC, and shall not be used for advertising or product endorsement purposes.

REFERENCES

1. MIT (2006), "The Future of Geothermal Energy: Impact of Enhanced Geothermal Systems (EGS) on the United States in the 21st Century" Rep., 372 pp, Massachusetts Institute of Technology.
2. Adachi, J., Siebrits, E., Peirce, A., and Desroches, J. (2007) "Computer simulation of hydraulic fractures", *International Journal of Rock Mechanics and Mining Sciences*, **44**: 739-757.
3. Johnson, S.M., Morris, J.P. (2009) "Model Development to Characterize Hydraulic Fracturing for Geologic Carbon Sequestration Applications." *International Conference on Rock Joints and Jointed Rock Masses*, Tucson, AZ.
4. Settgast, R.R, Rashid, M.M, (2009) "Continuum coupled cohesive zone elements for analysis of fracture in solid bodies", *Engineering Fracture Mechanics*, **76**, p. 1614-1635.
5. Xu XP, Needleman A. (1995), "Numerical simulations of dynamic crack growth along interface". *Int J Fracture*, **74(4)**:289–324.
6. Sam Chin-Hang, Papoulia KD, Vavasis SA. (2005) "Obtaining initially rigid cohesive finite element models that are temporally convergent." *Engng Fract Mech*, 2005; **72**:2247–57.
7. Fu, P., Johnson, S.M., Settgast, R.R., and Carrigan, C.R. (2011). "Generalized displacement correlation method for estimating stress intensity factors." *Engineering Fracture Mechanics*, in review.
8. Vorobiev, O. (2011), "Simple Common Plane Algorithm", *International Journal of Numerical Methods in Engineering*,
9. Fu, P., Johnson, S.M., Hao, Y., and Carrigan, C.R. (2011) "Fully coupled geomechanics and discrete flow network modeling of hydraulic fracturing for geothermal applications." *The 36th Stanford Geothermal Workshop*, Jan. 31 – Feb. 2, 2011, Stanford, CA.
10. Lin, W;Blair, S C;Wilder, D;Carlson, S;Wagoner, J;DeLoach, L;Danko, G;Ramirez, A L; Lee, K. (2001), "Large Block Test Final Report", UCRL-ID-132246-REV-2. 442pp.